



An expert system for the diagnosis of faults in rotating machinery using adaptive order-tracking algorithm

Jian-Da Wu^{a,*}, Mingsian R. Bai^b, Fu-Cheng Su^b, Chin-Wei Huang^c

^a Institute of Vehicle Engineering, National Changhua University of Education, 1 Jin-De Road, Changhua City, Changhua 500, Taiwan, ROC

^b Department of Mechanical Engineering, National Chiao-Tung University, Hsin-Chu, Taiwan, ROC

^c Department of Mechanical and Automation Engineering, Da-Yeh University, Changhua, Taiwan, ROC

ARTICLE INFO

Keywords:

Signal processing
Fault diagnosis
Order-tracking
Adaptive RLS filter

ABSTRACT

This paper describes an application of an adaptive order-tracking technique for the diagnosis of faults in rotating machinery. Conventional methods of order-tracking are primarily based on Fourier analysis with reference to shaft speed. Unfortunately, in some applications of order-tracking performance is limited, such as when a smearing problem arises and also in a multiple independent shaft system. In this study, the proposed fault diagnostic system is based on a recursive least-square (RLS) filtering algorithm. The problem is treated as the tracking of various frequency bandpass signals. Order amplitudes can be calculated with high-resolution in real-time implementation. The algorithm is implemented on a digital signal processor (DSP) platform for diagnosis and evaluated by experimental investigation. An experimental investigation is implemented to evaluate the proposed system in two applications of gear-set defect diagnosis and in the diagnosis of damaged engine turbocharger blades. The results of the experiments indicate that the proposed algorithm is effective in fault diagnosis for both experimental cases. Furthermore, a characteristic analysis and experimental comparison of a vibration signal and a sound emission signal for the present algorithm are also presented in this report.

© 2008 Elsevier Ltd. All rights reserved.

1. Introduction

Traditionally, the condition of rotating machinery such as fans, compressors, motors and engines can be monitored by measuring the respective vibration signal or sound emission signal. These signals normally consist of a combination of the basic frequency with discrete or narrowband frequency components and the harmonics thereof, most of which are related to the revolution of the machinery. The sound emission and vibration energy are increased when the machinery is damaged. An example result of a sound emission power spectrum level measured from the wheel-blades of an internal combustion (IC) engine turbocharger is shown in Fig. 1. The conventional fault diagnostic technique is to observe the amplitude difference in the time or the frequency domain for diagnosis of damage.

Recently, the order-tracking technique has become an important approach for diagnosing fault in rotating machinery. Interest in diagnosis using the order-tracking technique has grown significantly, having advanced with the progress of digital signal processing algorithms and technology in the last two decades (Biswas, Pandey, Bluni, & Samman, 1994; Chen, Du, & Qu, 1995; Gelle, Colas,

& Serviere, 2001; Lin & Qu, 2000; Shibata, Takahashi, & Shirai, 2000). The conventional order-tracking method is primarily based on Fourier analysis with reference to shaft revolution (Lee & White, 1998; Vold & Leuridan, 1993). Unfortunately, re-sampling processing is generally required in the fast Fourier transform (FFT) methods to compromise between time and frequency resolution for varying revolutions. However, in the conventional FFT methods, a smearing problem generally arises in practical implementation, particularly at low revolution speeds. In addition, the conventional methods are ineffective for application to certain critical conditions such as a fixed sampling frequency, and FFT analysis with a tracking technique is ineffective when the shaft speed varies rapidly.

In this study, an adaptive order-tracking fault diagnostic technique using both vibration signals and sound emissions is applied to the diagnosis of damage in gear-sets and engine turbocharger blades. According to recent studies by Haykin (1996) and Bai, Jeng, and Chen (2002) there exists some conclusions for adaptive filtering algorithms and their application to order-tracking techniques. The proposed adaptive fault diagnostic system is based on the recursive least-square (RLS) algorithm (Bai et al., 2002). Similar to conventional methods, the RLS method also requires information on shaft or engine revolution. The algorithm is essentially sample-based; thus, order amplitudes can be calculated in a real-time fashion. The method is well suited for high-resolution

* Corresponding author.

E-mail address: jdwu@cc.ncue.edu.tw (J.-D. Wu).

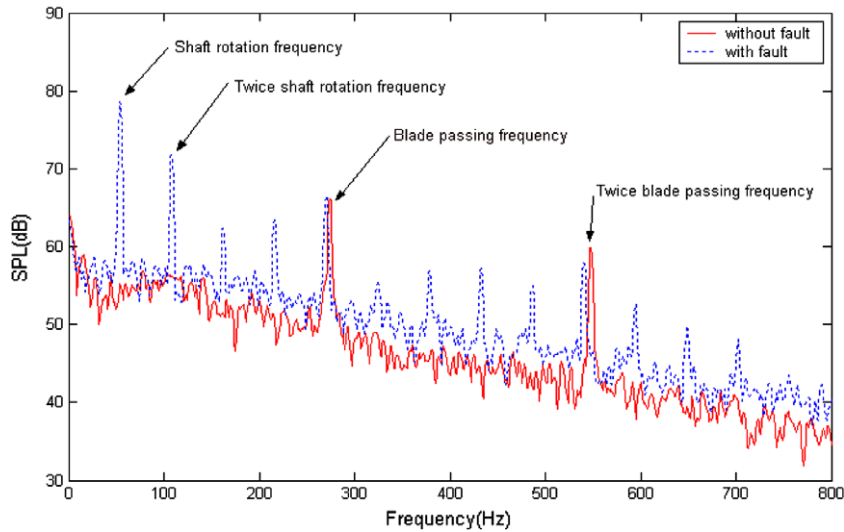


Fig. 1. Sound power spectrum level of sound emissions from turbocharger blades. A solid line depicts blades without damage; broken lines depict blades of which one is damaged.

tracking of closely spaced orders or crossing orders. The filter algorithm is implemented in a TMS320C32 DSP platform for evaluating the performance in a practical application of the diagnosis of damage in gear-sets and IC engine turbocharger blades.

In fault diagnostic techniques to date, measurement of the vibration signal has become most widely used when a reference signal is available. Unfortunately, in some practical applications, such a vibration signal is unavailable. Measurement of high-frequency sound emissions serves as a promising alternative to condition monitoring of many types of rotating machinery (Mba, 2002; Toutountzakis & Mba, 2003). During operation of the machinery, defects at different locations will generate characteris-

tic frequencies. However, in the present study, both vibration signals and sound emission signals are used to evaluate the proposed diagnostic technique. The details of the proposed adaptive filtering with an RLS algorithm are described in the following section.

2. Principle of adaptive order-tracking technique using RLS algorithm

The conventional algorithms used in fault diagnostic techniques fall into two categories. One is Fourier transform with a fixed sampling rate for obtaining frequency domain information; the other is

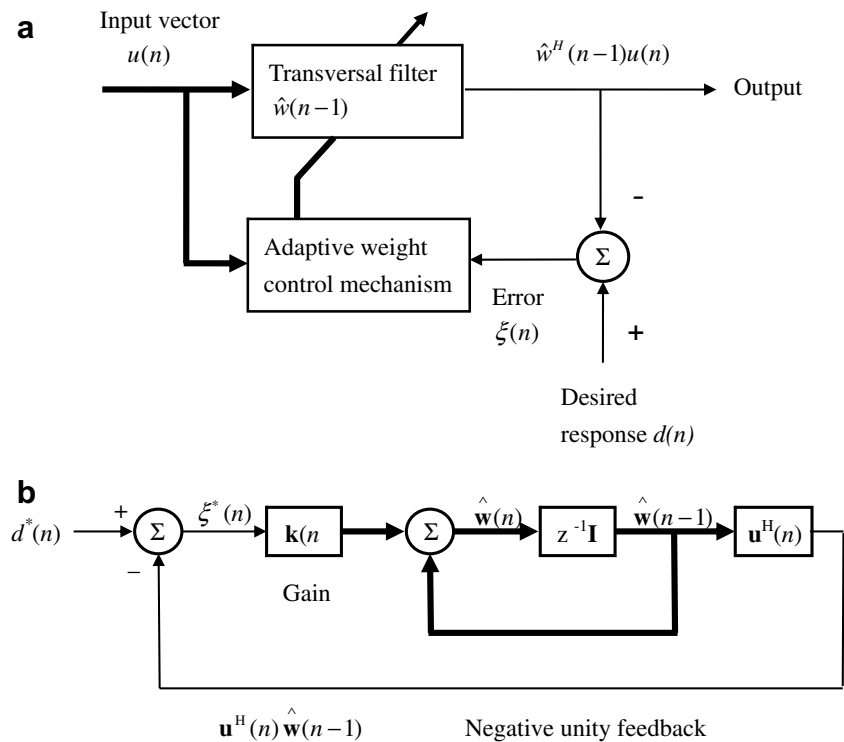


Fig. 2. Representations of RLS algorithm. (a) Block diagram and (b) signal-flow graph.

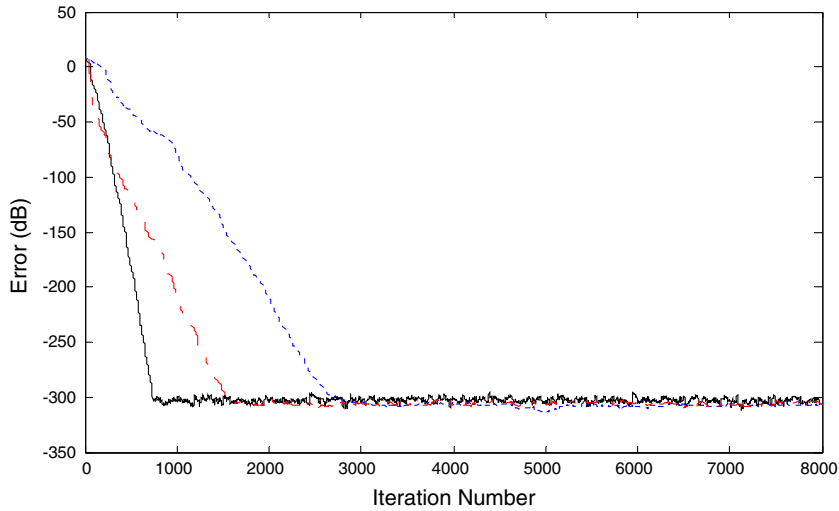


Fig. 3. A comparison of convergence speeds and estimation errors in various adaptive filters. A solid line depicts the Kalman filter; a dash-dot line depicts the RLS; a dotted line depicts the LMS.

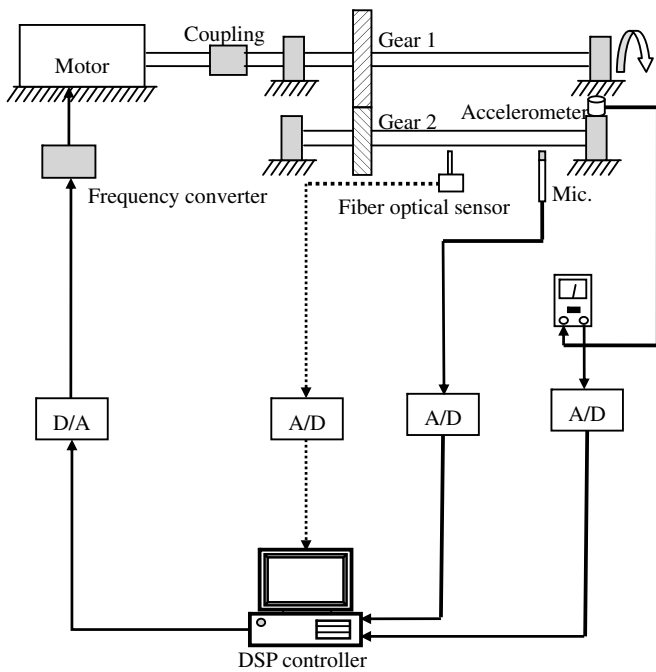


Fig. 4. Experimental arrangement of gear-set defect diagnosis.

tracking with various sampling rates. The second method employs a re-sampling scheme synchronous with the shaft revolution. The time domain data are hence converted to revolution-domain data. Then the FFT is also applied to obtain the order spectrum with respect to engine speed. Both the time and the frequency resolution of this approach are essentially varied with the shaft speed. This FFT order-tracking method relies on accurate measurement of the tachometer signal. In general, the vibration signal or the sound emission signal generated by rotating machinery essentially consists of a combination of the basic frequency with narrowband frequency components and its harmonic frequencies, most of which are related to the revolution of the machine. Bai et al. (2002) proposed an RLS algorithm for adaptive order-tracking technique. In this work, the vibration signal $x(t)$ containing k orders generated by one rotating shaft can be written as

$$x(t) = [\cos[\theta(t)] - \sin[\theta(t)] \cos[2\theta(t)] - \sin[2\theta(t)] \cdots \cos[k\theta(t)] - \sin[k\theta(t)]] \begin{bmatrix} A_{1I} \\ A_{1Q} \\ A_{2I} \\ A_{2Q} \\ \vdots \\ A_{kI} \\ A_{kQ} \end{bmatrix} \quad (1)$$

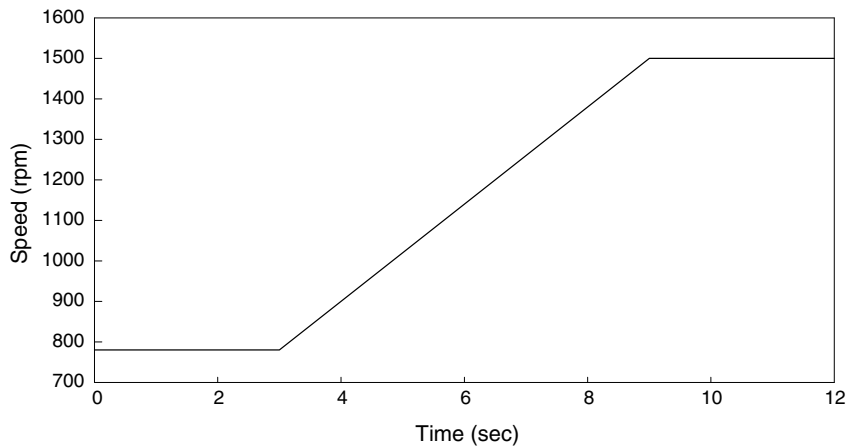


Fig. 5. Revolution of gear-set in experimental case.

where A_{kl} and A_{kQ} denote the in-phase and quadrature components, respectively, of k th order. Note that

$$A_{kl} = A_k \cos \phi_k, \quad A_{kQ} = A_k \sin \phi_k. \tag{2}$$

The amplitude of k th order can be written as

$$|A_k| = \sqrt{A_{kl}^2 + A_{kQ}^2}. \tag{3}$$

and the phase of the k th order is obtained by

$$\phi_k = \tan^{-1} \left(\frac{A_{kQ}}{A_{kl}} \right). \tag{4}$$

For a discrete-time system, Eq. (1) can be expressed as

$$x(n) = [\cos[\theta(n)] - \sin[\theta(n)] \cos[2\theta(n)] - \sin[2\theta(n)] \cdots \cos[k\theta(n)] - \sin[k\theta(n)]] \begin{bmatrix} A_{1I} \\ A_{1Q} \\ A_{2I} \\ A_{2Q} \\ \vdots \\ A_{kI} \\ A_{kQ} \end{bmatrix} \tag{5}$$

where n is the discrete-time index (Oppenheim & Schaffer, 1999). To solve Eq. (5), collect $2k$ samples of $x(n)$ to form

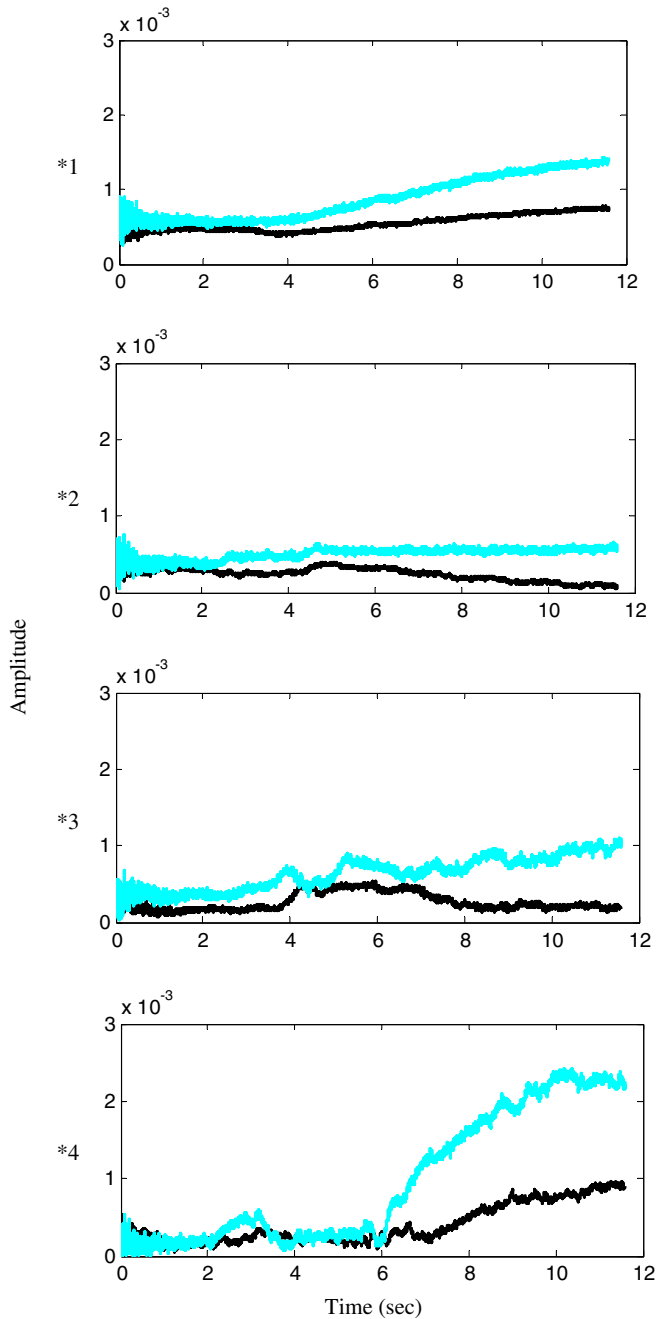


Fig. 6. Order figures of vibration signals for gear-set using adaptive RLS filter. A solid line depicts gear without defect; a dashed line depicts gear with a defect.

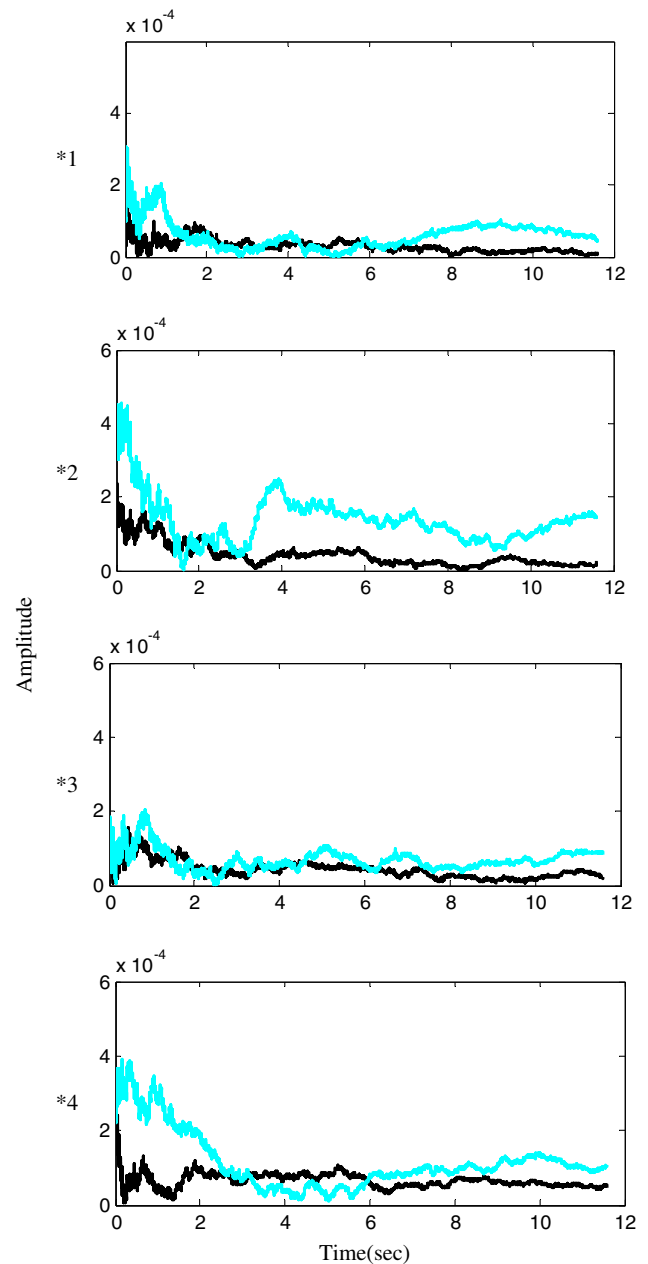


Fig. 7. Order figures of sound emission signals for gear-set using adaptive RLS filter. A solid line depicts gear without defect; a dashed line depicts gear with a defect.

$$\begin{bmatrix} x(n) \\ x(n+1) \\ \vdots \\ x(n+k) \\ x(n+2k-1) \end{bmatrix} = \begin{bmatrix} \cos[\theta(n)] & -\sin[\theta(n)] & \cdots & \cos[k\theta(n)] & -\sin[k\theta(n)] \\ \cos[\theta(n+1)] & -\sin[\theta(n+1)] & \cdots & \cos[k\theta(n+1)] & -\sin[k\theta(n+1)] \\ \vdots & \vdots & \cdots & \vdots & \vdots \\ \cos[\theta(n+2k)] & -\sin[\theta(n+2k)] & \cdots & \cos[k\theta(n+2k)] & -\sin[k\theta(n+2k)] \\ \cos[\theta(n+2k-1)] & -\sin[\theta(n+2k-1)] & \cdots & \cos[k\theta(n+2k-1)] & -\sin[k\theta(n+2k-1)] \end{bmatrix} \begin{bmatrix} A_{1I} \\ A_{1Q} \\ \vdots \\ A_{kI} \\ A_{kQ} \end{bmatrix} \quad (6)$$

Here it is assumed that the $2k$ amplitude parameters A_I and A_Q remain constant within the interval $[n, n + 2k - 1]$. In view of the special structure of the signal described in Eq. (1), the order-tracking problem can be recast into a parameter identification form. The estimation error

$$e(n) = x(n) - \mathbf{w}^T(n)\mathbf{u}(n), \quad (7)$$

$$\mathbf{u}^T(n) = [\cos[\theta(n)] - \sin[\theta(n)] \cos[2\theta(n)] - \sin[2\theta(n)] \cdots \cos[k\theta(n)] - \sin[k\theta(n)]] \quad (8)$$

is the regressor;

$$\mathbf{W}^T(n) = [A_{1I}(n) \ A_{1Q}(n) \ A_{2I}(n) \ A_{2Q}(n) \ \cdots \ A_{kI}(n) \ A_{kQ}(n)] \quad (9)$$

is the parameter vector; $x(n)$ is the measurement error. Note that the vector $\mathbf{u}(n)$ consists of angular displacements of the shaft; the

vector $\mathbf{w}(n)$ consists of the in-phase and quadrature components of all orders to be identified.

The parameter identification problem in Eq. (7) can be solved by the method of least-squares (Denbigh, 1998). The problem amounts to finding optimal parameters $\mathbf{w}(n)$ so that the performance index $\zeta(n)$ is minimized as

$$\zeta(n) = \sum_{i=1}^n \lambda^{n-i} |e(i)|^2, \quad (10)$$

where the forgetting factor λ exponentially weighs the estimation error from the present to the past. Fig. 2 shows the block diagram and signal-flow graph of the RLS algorithm. The optimal solution of the problem can be recursively solved by using the following RLS algorithm (Haykin, 1996):

$$\mathbf{k}(n) = \frac{\lambda^{-1}\mathbf{P}(n-1)\mathbf{u}(n)}{1 + \lambda^{-1}\mathbf{u}^H(n)\mathbf{P}(n-1)\mathbf{u}(n)} \quad (11)$$

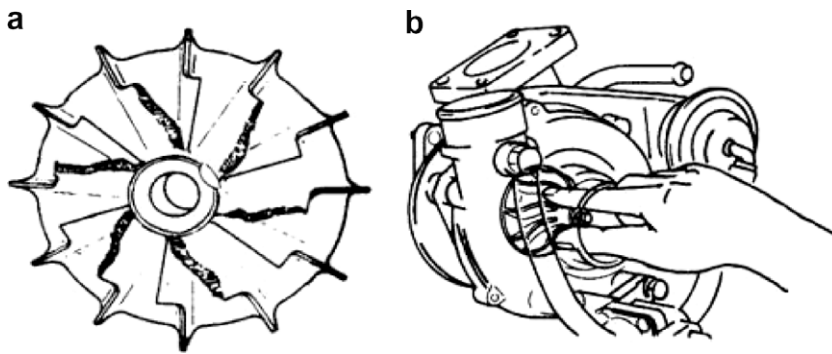


Fig. 8. (a) Damaged turbocharger compress-wheel-blades. (b) Make sure that turbocharger shaft-wheel assembly turns freely and smoothly by rotating it by hand (Crouse & Anglin, 1993).

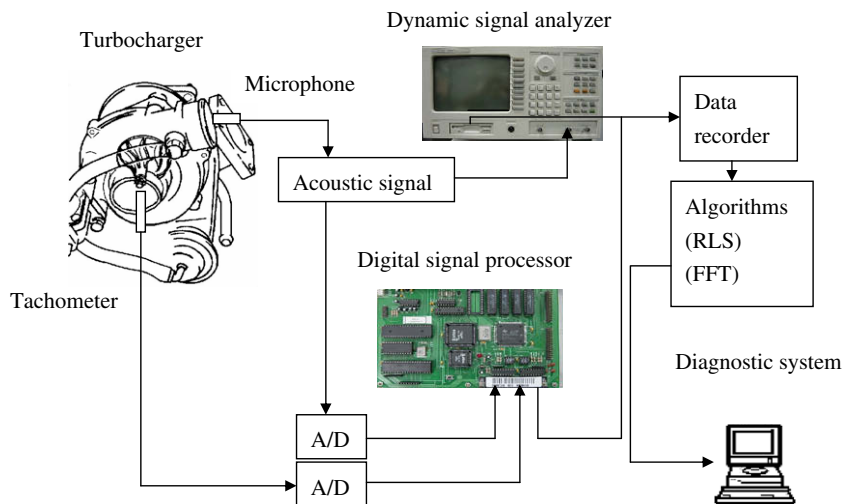


Fig. 9. Experimental arrangement for diagnosis of turbocharger wheel-blade faults.

$$\xi(n) = d(n) - \hat{\mathbf{w}}^H(n-1)\mathbf{u}(n), \tag{12}$$

$$\hat{\mathbf{w}}(n) = \hat{\mathbf{w}}(n-1) + \mathbf{k}(n)\xi^*(n), \tag{13}$$

$$\mathbf{P}(n) = \lambda^{-1}\mathbf{P}(n-1) - \lambda^{-1}\mathbf{k}(n)\mathbf{u}^H(n)\mathbf{P}(n-1). \tag{14}$$

In this procedure, matrix $\mathbf{P}(n)$ is the inverse of the auto-correlation matrix of input vector \mathbf{u} , $\xi(n)$ is the *a priori* estimation error, and $\mathbf{k}(n)$ is the gain vector. To initialize the RLS algorithm, the initial conditions are generally taken to be $\hat{\mathbf{w}}(0) = \mathbf{0}_{M \times 1}$, where M is the number of parameters and $\mathbf{P}(0) = \delta^{-1}\mathbf{I}$, where \mathbf{I} is an $M \times M$ identity matrix and δ is a small positive constant. One reason for using the RLS order-tracking technique is that the rate of convergence of the RLS algorithm is typically an order of magnitude faster than the traditional LMS algorithm.

In order to provide valid understand of the characteristic in adaptive filtering algorithms. A comparison of convergence speeds and the mean-square-error (MSE) in various adaptive filters, i.e.,

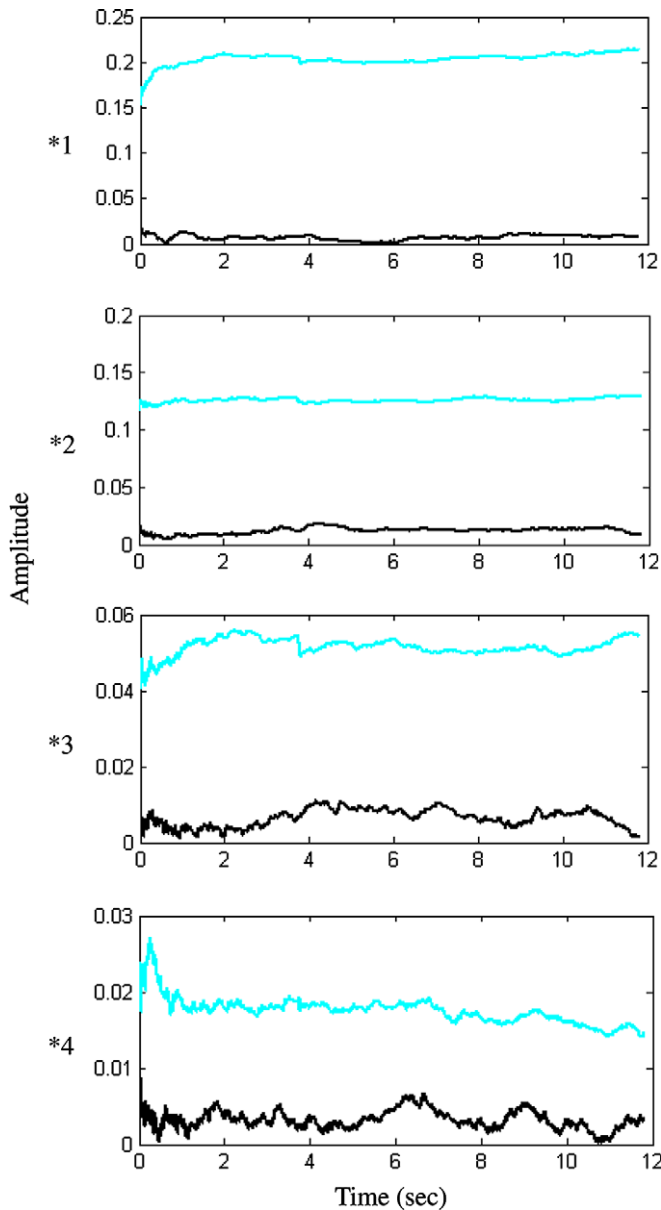


Fig. 10. Order figures of sound emission signals for engine speed at 800 rpm using adaptive RLS filter. A solid line depicts blades without any damage; dashed line depicts blades with one fault.

LMS, RLS, and Kalman filter in simulation is shown as Fig. 3. The results have shown that the Kalman filter has the quickest convergence speed, converging at the iteration number of 800, the RLS converges at 1500, and LMS converges at 2800. That is because the Kalman filter algorithm takes into account the noise factor and is well structured with sophisticated considerations. However, the Kalman filter may be exploited as the basis for deriving an adaptive filtering algorithm appropriate to the complex calculation situations. In particular, each updated estimate of the state is computed from the previous estimate and the new input data, so the previous estimate requires storage. Comparatively, the RLS filter algorithm is rather simple in filtering design.

3. Experimental verification of fault diagnostic systems

In the experimental investigation, two experiments are implemented to evaluate the proposed RLS filtering algorithm. One is a gear-set defect diagnosis using both the vibration signal and the sound emission signal; the other is a diagnosis of damaged IC engine turbocharger wheel-blades by using a sound emission signal.

3.1. Application 1: gear-set defect diagnosis

The experimental setup for the gear-set defect diagnostic system is shown in Fig. 4. The horsepower of the DC servo motor is 0.5 with a maximum revolution of 3000 rpm. The motor can be controlled by using a DSP controller. An optical fiber sensor (LM339) is used to detect motor revolution and angular displacement as reference signals in the diagnostic system. The vibration signal and sound emission are measured by using an accelerometer (PCB 353B15) and a condenser microphone (ACO P4012). The proposed diagnostic system is implemented on a 60 MHz floating-point TMS320C32 DSP equipped with two 16-bit analog I/O channels by using the adaptive RLS algorithm. In applying the proposed high-resolution order-tracking methods, some parameters need to be determined, such as the number of tracking orders N_{order} and forgetting factor λ in the proposed RLS algorithm.

In addition, the experimental implementation of the gear-set is at various speed conditions. The experimental conditions are indicated in Fig. 5, where the gear-set is operated as a running-up schedule. The experimental results from order figures using a vibration signal are shown in Fig. 6; the order figures using a sound

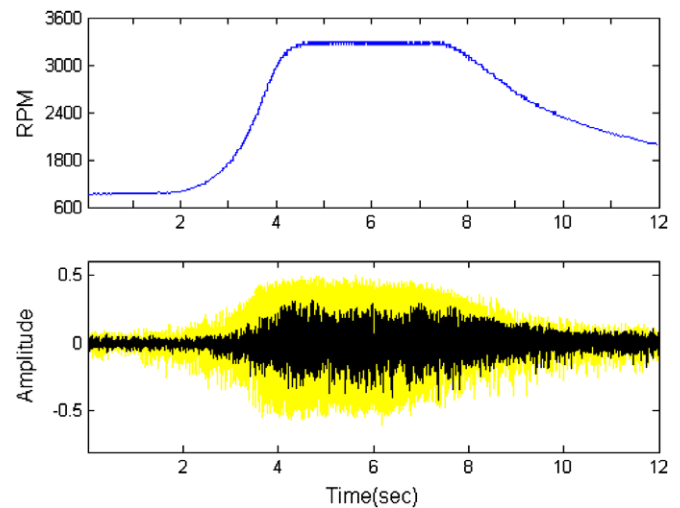


Fig. 11. Sound pressure amplitude in test schedule for diagnosis of faults in turbocharger blades. A solid line depicts blades without any damage; a dashed line depicts blades with one fault.

emission signal are shown in Fig. 7. The experimental results demonstrate that the proposed diagnostic system is effective in defect diagnosis by using both vibration and sound emission signals. The ordered figures can be saved as a data bank for practical fault diagnosis. Furthermore, order-tracking is one of the important tools for feature extraction of rotating machinery. The order amplitude figure gives the information of the harmonic order signal in the mechanical system. Ordinarily, the amplitude of fault conditions is higher than without fault condition. So it is very easy to distinguish the fault and without fault conditions.

3.2. Application 2: diagnosis of damaged IC engine turbocharger wheel-blades

An IC engine can produce more power at the same speed if a forced induction system is used to improve volumetric efficiency. Such a system consists of air pumps or blowers that force more

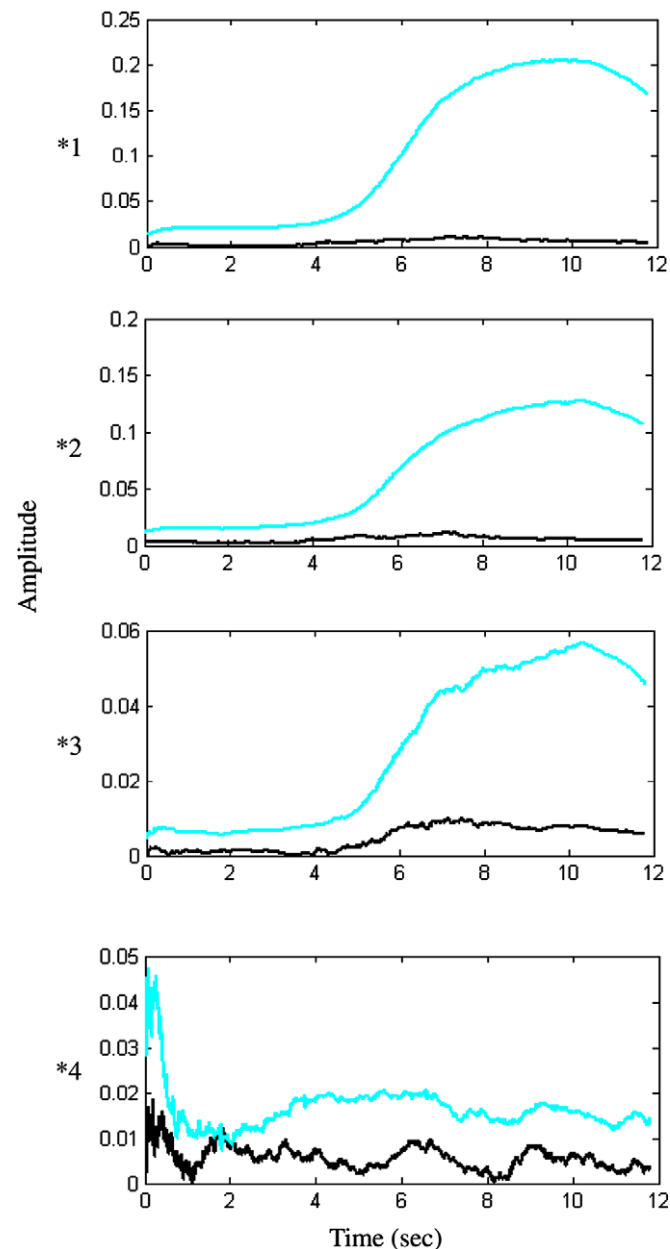


Fig. 12. Order figures of sound emission signals for engine run-up test. A solid line depicts blades without any damage; a dashed line depicts blades with one fault.

air-fuel mixture into the engine combustion chamber. Normally they may produce 35–60% more power than a naturally-aspirated engine (Crouse & Anglin, 1993). However, the turbocharger system requires periodic maintenance to prevent early failure. Frequent causes of turbocharger failure are sand and other particles striking the blades, as in the case of the turbo blades shown in Fig. 8a. Conventional diagnosis of damaged blades is to conduct a visual inspection when the engine is cool or check to make sure that the turbocharger shaft-wheel assembly turns freely and smoothly by rotating it by hand, as shown in Fig. 8b. Obviously, the conventional inspection is not a precision approach for diagnosis of damage; it also is not a suitable method for diagnosis when the engine is running. The conventional FFT methods with a fixed sampling frequency also are ineffective for this application because normal operation of the engine varies rapidly.

In fault diagnostic techniques to date, the vibration signal has become the most widely used method when a vibration signal is available. Unfortunately, in some applications of fault diagnostic systems, a vibration reference signal is unavailable. In this application, only the sound emission signal is used to evaluate the proposed system in the diagnosis of a damaged turbocharger under fixed revolution, acceleration and deceleration conditions. The experimental arrangement for the diagnosis of damaged turbocharger wheel-blades is depicted in Fig. 9. A four-cylinder, four-stroke, 2.8-l IC engine with a turbocharger system is used in this application. A fiber-optic sensor is utilized to detect the revolution signal that is related to the sound emission from the wheel-blades. In this experimental implementation, the related reference signal from the engine can be measured by the ignition system or the wheel-blade signal. However, the ignition system may have substantial interference that will affect the performance; therefore, the reference signal is picked up near the wheel-blades by using a fiber-optic sensor. To verify the filtering algorithm in order-tracking, a preliminary test was conducted in an engine with a fixed revolution of 800 rpm. The order figures using a sound emission signal are shown in Fig. 10. In a practical condition, an engine may be operated by running-up or casting down. Although the high sweep rates make accurate order measurement difficult, the proposed adaptive order-tracking is suitable for such a condition. In order to verify the adaptive filter, the test schedule for the diagnosis of damaged turbocharger blades is shown in Fig. 11. The ordered figures using a sound emission signal are shown in Fig. 12. The experimental results demonstrate that the proposed diagnostic system is effective in fault diagnosis by using sound emission signals. The ordered figures and data also can be saved as a data bank for practical fault diagnosis.

4. Conclusions

An order-tracking technique exploiting adaptive filtering based on an RLS algorithm for tracking the orders of vibration and sound emission signals in the diagnosis of defects in a gear-set and in damaged engine turbocharger wheel-blades has been applied. In this method, the order-tracking problem was treated as parameter identification and calculated at a high-resolution. Although, the Kalman filter is the alternative method when the uncertainty factors of the entire system are taken into consideration. However, in some cases the design is more complex than the RLS algorithm. In the present study, the contribution is emphasized in the practical application of gear-set defect diagnosis and diagnosis of damaged IC engine turbocharger wheel-blades by using the proposed RLS filtering algorithm. The results of the experiments indicated that the RLS algorithm is effective in fault diagnosis for both experimental cases. Various adaptive filtering algorithms are expected to be used in different applications; future research should focus on

the development of a robust adaptive filtering algorithm to accommodate perturbation as well as uncertainties in the diagnostic system.

Acknowledgements

This study was supported by the National Science Council of Taiwan, the Republic of China, under project number NSC-93-2212-E-018-004. The authors also wish to express appreciation to Dr. Cheryl Rutledge for her editorial assistance.

References

- Bai, M. R., Jeng, J., & Chen, C. (2002). Adaptive order tracking technique using recursive least-square algorithm. *Transactions of the ASME, Journal of Vibrations and Acoustics*, 124, 502–511.
- Biswas, M., Pandey, A. K., Bluni, S. A., & Samman, M. M. (1994). Modified chain-code computer vision techniques for interrogation of vibration signatures for structural fault detection. *Journal of Sound and Vibration*, 175, 89–104.
- Chen, Y. D., Du, R., & Qu, L. S. (1995). Fault features of large rotating machinery and diagnosis using sensor fusion. *Journal of Sound and Vibration*, 188, 227–242.
- Crouse, W. H., & Anglin, D. L. (1993). *Automotive mechanics*. McGraw-Hill.
- Denbigh, P. (1998). *System analysis and signal processing*. Addison Wesley.
- Gelle, G., Colas, M., & Serviere, C. (2001). Blind source separation: a tool for rotating machine monitoring by vibration analysis. *Journal of Sound and Vibration*, 248, 865–885.
- Haykin, S. (1996). *Adaptive filter theory*. Prentice-Hall.
- Lee, S. K., & White, P. R. (1998). The enhancement of impulsive noise and vibration signals for fault detection in rotating and reciprocating machinery. *Journal of Sound and Vibration*, 217, 485–505.
- Lin, J., & Qu, L. (2000). Feature extraction based on morlet wavelet and its application for mechanical fault diagnosis. *Journal of Sound and Vibration*, 234, 135–148.
- Mba, D. (2002). Applicability of acoustic emissions to monitoring the mechanical integrity of bolted structures in low speed rotating machinery: Case study. *NDT and E International*, 35(5), 293–300.
- Oppenheim, A. V., & Schaffer, R. W. (1999). *Discrete-time signal processing*. Prentice-Hall.
- Shibata, K., Takahashi, A., & Shirai, T. (2000). Fault diagnosis of rotating machinery through visualization of sound signals. *Mechanical Systems and Signal Processing*, 14, 229–241.
- Toutountzakis, T., & Mba, D. (2003). Observations of acoustic emission activity during gear defect diagnosis. *NDT and E International*, 36, 471–477.
- Vold, H., & Leuridan, J. (1993). High resolution order tracking at extreme slew rates, using Kalman filters. SAE Paper 931288 (pp. 219–226)..